TELKOMNIKA Telecommunication Computing Electronics and Control
Vol. 22, No. 4, August 2024, pp. 1005~1014
ISSN: 1693-6930, DOI: 10.12928/TELKOMNIKA.v22i4.25883

End-fire multibeam radial line slot array antennas

Teddy Purnamirza[1], Junisbekov M. Shardarbekovich[2], Riza A. Jaya[1], Imran Mohd Ibrahim[3], Kabanbayev A. Batyrbekovich[2], Depriwana Rahmi[4]
[1]Department of Electrical Engineering, Universitas Islam Negeri Sultan Syarif Kasim, Pekanbaru, Indonesia
[2]Department of Automation and Telecommunications, Taraz Regional University named after M. Kh. Dulaty, Taraz, Kazakhstan
[3]Department of Electronic Engineering, Universiti Teknikal Malaysia Malaka, Malaka, Malaysia
[4]Department of Mathematic Educations, Universitas Islam Negeri Sultan Syarif Kasim, Pekanbaru, Indonesia

Article Info

Article history:

Received Nov 28, 2023
Revised Jan 16, 2024
Accepted Feb 13, 2024

Keywords:

End-fire
High beamsquint
Multibeam
Radial line slot array
Wi-Fi

ABSTRACT

This research proposed and verified a novel method in realizing end-fire radial line slot array (RLSA) antennas. This method involved the use of high beamsquint values in the design of slot pairs, which aimed to shift the antenna's beam toward the end-fire direction. Furthermore, identical slot pairs were also placed in the antenna's background to further squint the beam in the end-fire direction. By using this method, forty multibeam end-fire RLSA antennas were modeled and simulated to determine the most efficient model to be fabricated. The accuracy of the simulations was confirmed through measurements taken from the fabricated prototype, which demonstrate good agreement with the simulation results and confirm the validity of the proposed method. The result showed that it is possible to design four end-fire beam antennas with a gain of 8 dBi, directions of 0°, 90°, 180°, and 270° in the azimuth direction, and a beamwidth of about 20°. The antenna also showed low reflection and bandwidth of about 500 MHz, which is suitable for Wi-Fi applications.

Corresponding Author:

Teddy Purnamirza
Department of Electrical Engineering, Universitas Islam Negeri Sultan Syarif Kasim
Pekanbaru, Indonesia
Email: tptambusai@uin-suska.ac.id

1. INTRODUCTION

Big radial line slot array (RLSA) antennas were initially developed for satellite broadcast applications at Ku-band frequency [1]-[4]. With the same size as parabolic antennas, RLSA antennas have similar gain while being superior in terms of low profile, feeder positions, and light weight [5]-[8]. Moreover, in year of 2022, the RLSA antennas were used as antennas for most advanced NASA satellites [9]-[12]. Due to its successful development, the RLSA antennas were then developed for small antenna applications such as antennas for Wi-Fi point-to-point devices at the frequency of 5.8 GHz. Although they initially had a problem with high signal reflection [13], the development gradually succeeded, particularly after the development of the extreme beamsquint technique that reduced the signal reflection effect [14]. Several RLSA antennas for Wi-Fi bridges adapted to market needs have been successfully developed and designed using this technique [14].

Using the extreme beamsquint technique, small RLSA antennas were successfully developed for multibeam applications [15], multibeam antennas created by utilizing background antennas to radiate [16]. Half- and one-third cut RLSA antennas were also developed for multibeam applications [17]. Additionally, a combination of cutting and the extreme beamsquint technique was successfully used to minimize the size of RLSA antennas [18].

As other broadside antenna types, RLSA antennas typically have a directional beam that points to the front of the antennas, as illustrated in Figure 1(a). In certain applications, it is necessary to have end-fire antennas, which have a beam pointing towards the side [19]-[24], as illustrated in Figure 1(b). Low-profile end-fire antennas are particularly suitable for use on vehicles, where the antenna's shape must be concealed, or on aircraft, where the antenna's shape can affect maneuverability. Since RLSA antennas are a type of low-profile antenna, it is interesting to develop RLSA antennas as end-fire antennas.

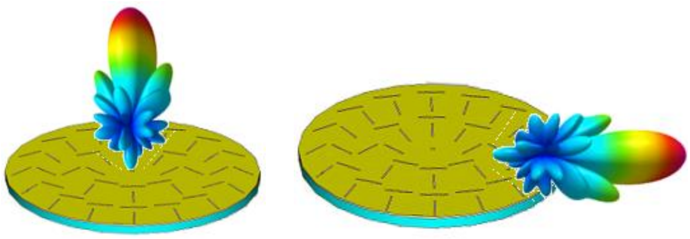

(a) (b)

Figure 1. Type of beam direction for RLSA; (a) broadside and (b) end-fire

This paper is the first to cover an end-fire RLSA antenna design. A technique for squinting the beam in the lowest elevation direction and a technique for using the antenna background to help pull the beam towards the end-fire direction are presented in section 2. The design parameters of RLSAs models and their feeders were discussed in section 3. Subsequently, an optimal model was fabricated, as detailed in section 4. Moreover, the measurement results of the fabricated prototype and the simulation results of the optimal model were analyzed, with a focus on parameters such as bandwidth, gain, beam direction, reflection coefficient, and beamwidth. The overall findings are summarized in section 5.

2. THE STRUCTURE OF BASIC BROADSIDE RLSA ANTENNAS

The basic structure of an ordinary RLSA consists of a copper radiating element, a polypropylene cavity, a copper background, and a feeder as shown in Figure 2(a). The radiating element is typically a circular plate made of metals, such as aluminum, copper, or brass, consisting of many slot pairs, with one slot pair acting as a single antenna element that radiates or receives signals. The distance between each slot pair is a multiple of the signal wavelength, causing the signals from all slot pairs to amplify each other, resulting in a signal gain. The background consists of a metal plate, similar to the radiating element, but devoid of any slots. The cavity, which takes the shape of a tube and is positioned alongside the radiating element and the background, serves as a dielectric material. This cavity functions as a circular waveguide, facilitating the transmission of signals from the feeder and guiding their propagation in the radial direction.

The feeder served the purpose of conveying signals from a transmission line to the antennas. This feeder, a conventional SMA feeder, was altered through the incorporation of a copper header, illustrated in Figure 2(b). The header's role is to transform electromagnetic power from a transverse electromagnetic (TEM) coaxial mode into a TEM cavity mode, specifically a radial mode. Consequently, the electromagnetic power supplied by the feeder is directed radially within the antenna cavity, as depicted in Figure 2(c). The feeder parameters, illustrated in Figure 2(d), were established via a parameterization process using a specialized C^{++} computer program top of form.

The slot pairs were determined and formulated utilizing (1) to (7) as outlined in references [1]-[3]. The meanings of the equations variables provided in Table 1 were taken from the same references and visually represented in Figure 3. Figure 3(a) depicts the meaning of variables of θ_1, θ_2, ϕ, ρ_1, ρ_2, and θ_T, while Figure 3(b) illustrates the meaning of variables of ϕ_T and θ_T. additionally, Figure 3(c) illustrate the meaning of variables of S_ρ and S_ϕ. Given the complexity of manually calculating the slots variables as well as drawing numerous slots and antennas structures of numerous antenna models, a visual basic application (VBA) computer program was developed and integrated within the CST computer software to enabled swift execution of the essential drawings and calculations. In (1) to (7) were used in the computer program to calculate slots parameters.

$$\theta_1 = \frac{\pi}{4} + \frac{1}{2}\left\{arctan\left(\frac{cos(\theta_T)}{tan(\emptyset_T)}\right) - (\emptyset - \emptyset_T)\right\} \tag{1}$$

$$\theta_2 = \frac{3\pi}{4} + \frac{1}{2}\left\{arctan\left(\frac{\cos(\theta_T)}{tan(\emptyset_T)}\right) - (\emptyset - \emptyset_T)\right\} \quad (2)$$

$$\rho_1 = \frac{(n-1+q-0.25)\lambda_g}{1-\xi sin\theta_T cos(\phi-\phi_T)} \quad (3)$$

$$\rho_2 = \frac{(n-1+q+0.25)\lambda_g}{1-\xi sin\theta_T cos(\phi-\phi_T)}\text{; where } \xi = \frac{1}{\sqrt{\varepsilon_{r_1}}} \quad (4)$$

$$S_\rho = \frac{\lambda_g}{1-\xi sin\theta_T cos(\phi-\phi_T)} \quad (5)$$

$$S_\phi = \frac{2\pi\lambda_g}{\sqrt{1-\xi^2 \sin{\theta_T}^2}} \frac{q}{p} \quad (6)$$

$$L_{rad} = (4.9876 \times 10^{-3}\rho)\frac{12.5\ x\ 10^9}{f_0} \quad (7)$$

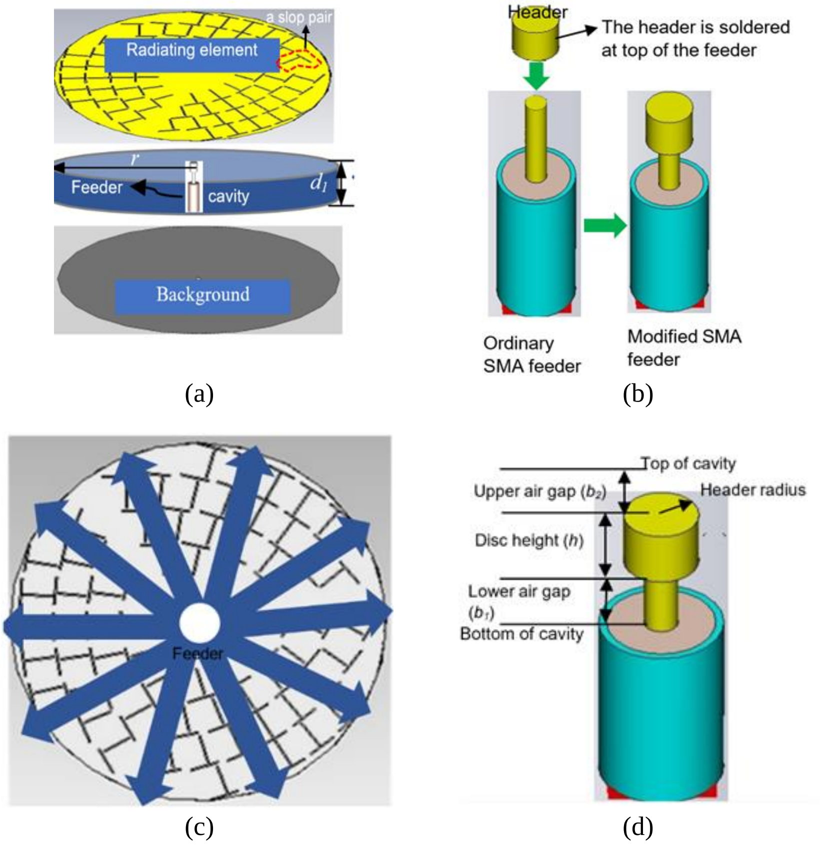

Figure 2. Illustration of; (a) the RLSA structure, (b) the placement of the copper header, (c) the power flow from the feeder to the antenna perimeter, and (d) the feeder parameters

Table 1. Design parameters of the slot pairs

Parameters	Symbols
The inclination angle of slot 1	θ_1
The inclination angle of slot 2	θ_2
Beamsquint angle in the elevation direction	θ_T
Azimuth angle of slot 1 and slot 2 position	ϕ
Beamsquint angle in azimuth direction	ϕ_T
Distance of slot 1 from the center point of antennas	ρ_1
Distance of slot 2 from the center point of antennas	ρ_2
Number of slot pairs in the first ring	n
Integer numbers (1, 2, 3…) that express the distance of the innermost ring from the center of the antennas	q
Distance between two adjacent unit radiators located in two different rings (distance in the radial direction)	S_ρ
Distance between two adjacent unit radiators in the same ring (distance in azimuth direction)	S_ϕ

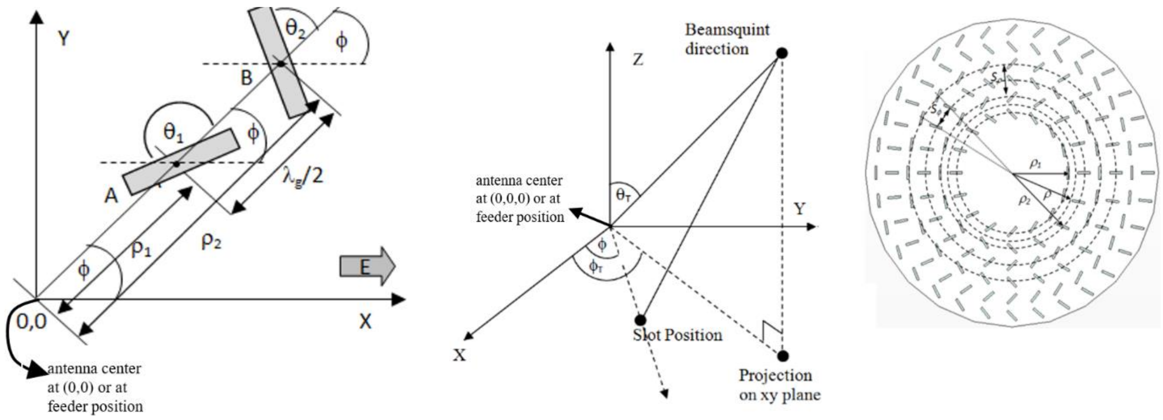

(a) (b) (c)

Figure 3. Visually representation of; (a) the parameters pertaining to the slots, (b) the positions of the slots and their correlations relative to the beam direction, and (c) the separation distance between slots in both the radial and azimuthal directions [25]

3. THE PROPOSED METHOD TO REALIZE END-FIRE RLSA ANTENNAS

In this research, a method was proposed to develop end-fire RLSA antennas, utilizing of two techniques. Those techniques are the high beamsquint technique and the utilization of antenna background technique. The high beamsquint technique is used to squint the beam to approach the end fire direction, while the utilization of antenna background is used to more squint the squinted beam to meet the end fire direction. The two techniques are discussed as follows.

3.1. Utilizations of high beamsquint values

Theoretically, end-fire RLSA antennas are possible to be realized by designing antenna slots using high beamsquint values such as 90° in elevation, which is the end-fire direction. However, the realized beamsquint will not be able to achieve 90° due to the emergence of grating beams. Figure 4(a) presents the simulation outcome, illustrating the correlation between the designed beamsquint (ranging from 60° to 90°) and the realized beamsquint values across various *n* values. The term “designed beamsquint” refers to the specific direction towards which the antenna is designed to squint its beam. This direction is typically determined during the antenna design phase and is based on the specific application requirements. On the other hand, the term “achieved beamsquint” refers to the actual direction towards which the designed antenna can squint its beam during operation. In summary, the “designed beamsquint” is the intended direction for the antenna’s beamsquint, while the “achieved beamsquint” is the actual direction that the antenna’s beamsquints towards during operation. From Figure 4(a), it can be observed that the maximum beamsquint direction that can be achieved is 70°, although RLSA antennas are designed for higher beamsquint directions (greater than 70°). Figure 4(b) is one of the simulation results of RLSA antennas designed using a high beamsquint of 89°, showing that the achieved beam is only about 70°.

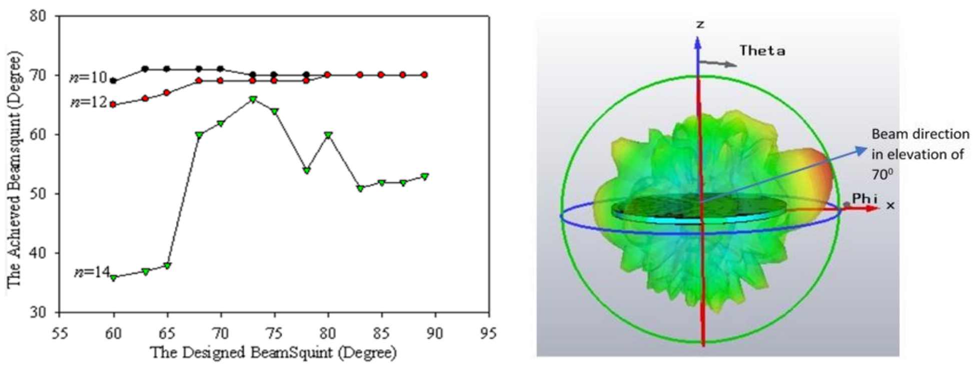

(a) (b)

Figure 4. Depicts; (a) the relationship between the intended beamsquint values and the actual beamsquint values achieved through simulation and (b) radiation pattern of an RLSA designed using beamsquint of 89°

Theoretically, the reason why high beamsquint values (greater than 70°) cannot be achieved is due to the emergence of grating beams. These grating beams exert an influence on the main beam's orientation, causing it to deviate from the originally intended direction. The amount of the grating beams will increase proportionally with the increase of the designed beamsquint direction. In (8) demonstrates the beamsquint direction (θ_T) that produces the grating beam [25].

$$\theta_T = sin^{-1}\left(\frac{\sqrt{\varepsilon_r}-1}{cos(\emptyset - \emptyset_T)}\right) \tag{8}$$

In the context of the simulation, the cavity's permittivity (ε_r) is set at 2.33. The minimal value of θ_T that triggers the generation of grating beams by the RLSA antenna's slots can be calculated by setting the beamsquint in azimuthal direction (θ_T) to 0° and the slot position in azimuth direction ($\emptyset$) to 0°. Employing (8) yields a results of θ_T= 31.8°. Additionally, from (8), it becomes evident that as θ_T surpasses 31.8°, other slots at their respective $\emptyset$ angles will begin to generate grating beams.

3.2. Utilization of antenna background

Since it is not possible to squint the antenna's beam into the end-fire direction using high beamsquint values, as discussed in the previous section, an alternative method is proposed. The utilization of the background to interfere with the beam is suggested, which results in a more squinted beam towards the end-fire direction. This is achieved by adding slots on the surface of the background, which are identical to the slots on the radiating element, as depicted in Figures 5(a) and (b). Although the utilization of the background for the placement of the slots is not typical since the background element usually functions only as a boundary waveguide. The resulting beam is a new beam that squinted to end-fire direction as illustrated in Figure 5(c) and therefore verifies the effectiveness of the proposed method in realizing end-fire beam for RLSA antennas. The antenna gain is 12 dBi, which is lower by about 1.7 dB than the gain of an identical size broadside RLSA antenna. The decrease gain of 1.7 dB is due to the high amount of grating beams as consequence of extremely squinting the antenna beam as discussed in the previous section.

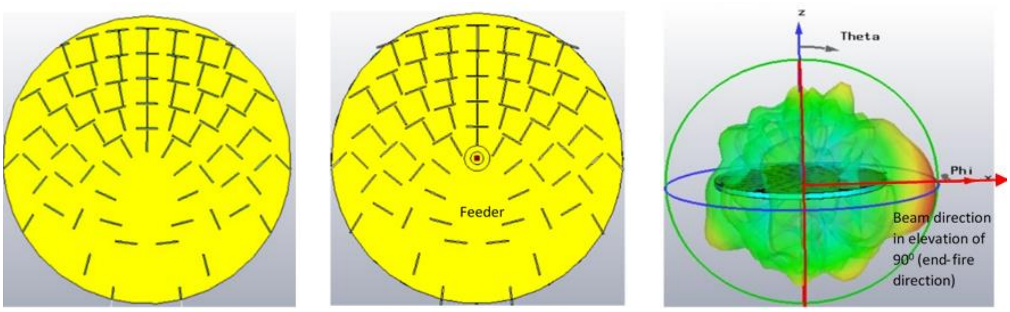

(a) (b) (c)

Figure 5. Design result of; (a) radiating element of the RLSA antennas, (b) background element of the RLSA antennas, and (c) radiation pattern of the RLSA antenna

4. DESIGNED ANTENNAS MODELS

Several antenna models were designed using the proposed techniques for high beamsquint (θ_T) varying from 70° to 90° with 3° increments, as well as for varying *n* values of 8, 10, 12, 14, and 16, obtaining forty antenna models. The variation aimed to get the best antenna model as well as to ensure the applicability of the developed technique in different values of *n* and θ_T. The parameter values for the antenna design and feeders are separately listed in Tables 2 and 3, respectively.

The antenna models were designed to have four end-fire beams pointing in four directions in azimuth (0°, 90°, 180°, and 270°) to accommodate the needs of future multibeam antennas. To achieve the multibeam, the antenna slots were grouped into four different groups, as depicted in Figure 6(a). For each group, identical slots were designed on the radiating element and on the background (as depicted in Figures 6(a) and (b)). Based on simulation results in Figures 6(c) and (d), four similar beams for different end-fire directions can be produced using the proposed techniques.

After simulating all 40 models, the best model was selected and fabricated, which has characteristics of p_0 and beamsquint (θ_T) of 12 and 87°, respectively. Subsequently, the fabricated prototype underwent measurements within an anechoic chamber to acquire data for gain and radiation patterns. Additionally, a network analyzer was employed to capture the reflection coefficient response. Figures 7(a) and (b) visually present the prototype and the corresponding measurement processes. The measurement outcomes were utilized to validate the simulation results, as detailed in the subsequent section.

Table 2. Parameters of the antenna models [17]

Symbol	Parameter	Value
ε_{r1}	Cavity permittivity	2.33
θ_T	Beamsquint angle	60° up to 89°
f	Frequency center	5.8 GHz
d	Background plane thickness	0.1 mm
d_1	Cavity thickness	8 mm
d_2	Radiating element thickness	0.1 mm
w	Slot width	1 mm
r	Antenna radius	115 mm
n	Number of slot pairs in the first ring	10, 12, 14, 16

Table 3. Specification parameters of the feeder [14]

Symbol	Parameter	Value (mm)
b_1	lower air gap	4
h	disc height	3
r_a	disc radius	1.4
b_2	upper air gap	1

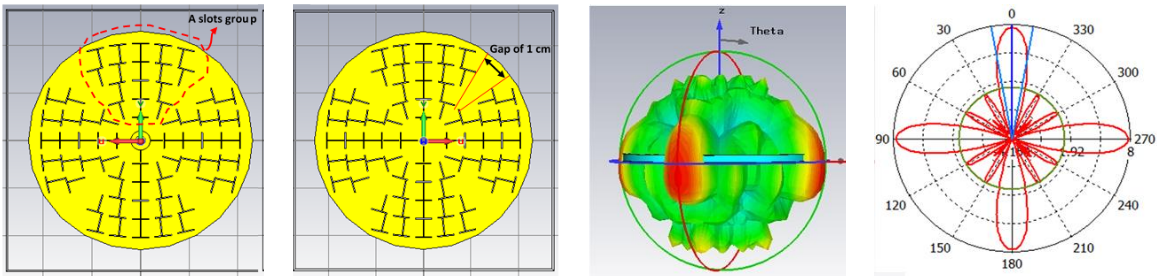

(a) (b) (c) (d)

Figure 6. Four identical slots groups on; (a) the radiating element, (b) the background element; resulted in 4 end-fire beams, (c) 3-dimension, and (d) 2-dimension in the azimuth plane

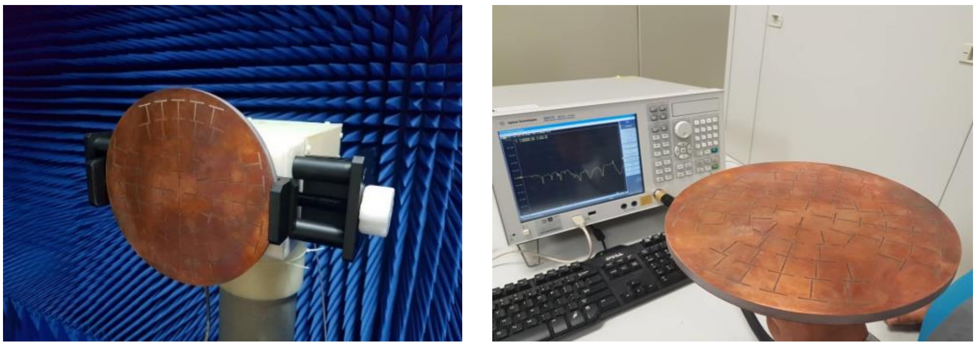
(a) (b)

Figure 7. Measurement of the prototype: (a) within the anechoic chamber and (b) employing a network analyzer

5. RESULT AND DISCUSSION

The antenna reflection coefficient for the measurement and simulation is shown in Figure 8. From the figure, the measured bandwidth was about 500 MHz (from 5.5 GHz to 6 GHz). This bandwidth is quite wide and enough for Wi-Fi applications since the required bandwidth only about 125 MHz.

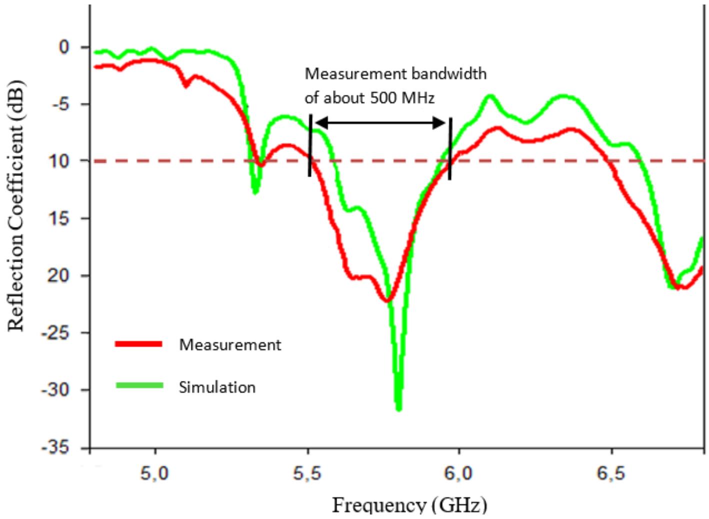

Figure 8. The reflection coefficient of the antenna

The antenna radiation pattern for the measurement and simulation is shown in Figure 9. From the figure, it is evident that the antenna exhibits four beams oriented approximately at 0°, 90°, 180°, and 270° azimuth angles, demonstrating a relatively symmetrical distribution. Additionally, the antenna features a consistent beamwidth of approximately 20° for each beam. To achieve uniformity and symmetry in the beams, a similar number of slots and positions were designed for each beam.

In order to mitigate potential coupling effects that could lead to gain reduction, an adequate gap was implemented, as depicted in Figure 6(b). This gap's size needed to be optimized to strike a balance: it should not be overly large to prevent excessive gain reduction, nor too small to prevent interference between neighboring beams. Consequently, a parameterization was executed to determine the optimal 1 cm gap value.

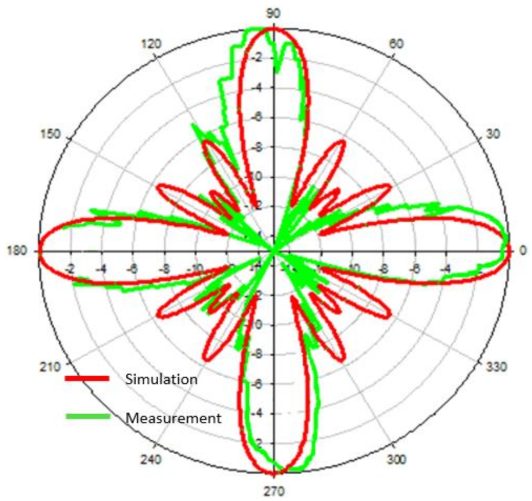

Figure 9. The radiation pattern of the antenna in the azimuth direction

Additionally, it's noticeable that all beams, as observed in both simulations and measurements, exhibit gains of approximately 8 dBi. This uniform gain across all beams signifies a well-balanced distribution of gain among them. In order to evaluate the decrease in gain compared to single-beam antennas, a single-beam RLSA antenna was designed for analysis. The simulation of this model yielded a gain of 15.9 dBi for the single-beam antenna. Theoretically, the gain of the multi-beam antenna should be lower than that of the single-beam by 6 dB, a consequence of the beam splitting into four directions. Therefore, the gain of 8 dBi for the multibeam antenna is lower by 1.9 dB than the expected gain of 9.9 dBi. This decrease in gain compensates for the conversion of the beam's original direction (bore-sight) to the end-fire direction.

Figures 8 and 9 present the congruencies observed between the measurement and simulation outcomes. Any minor disparities noted between these results can be attributed to imperfections in the prototype fabrication process. These imperfections primarily encompass aspects such as inaccuracies in printing the design of the radiating element, the placement of the antenna's feeder hole during drilling, and the precise positioning of the head disc during soldering.

6. CONCLUSION

This research has successfully developed a novel method for end-fire RLSA antennas. This method consists of two techniques: i) the use of high beamsquint to direct the beam towards the end-fire direction and ii) the placement of slot pairs on the antenna's background surface to further direct the beam towards the end-fire direction. This method is expected to contribute to the successful development of end-fire RLSA antennas for implementation in several applications that need low-profile end-fire antennas, such as in car and aircraft. In the future, this method can be further developed to create end-fire RLSA antennas with different numbers of beams or antenna sizes. A comparison between end-fire RLSA and end-fire microstrip also could be carried out in order to study the advantages and disadvantages of both types of antennas.

ACKNOWLEDMENTS

The authors appreciate the Lembaga Penelitian dan Pengabdian kepada Masyarakat (LPPM), Universitas Islam Negeri Sultan Syarif Kasim, Riau, Indonesia for partially funding this research. They also extend this appreciation to the Advanced Microwave Laboratory, Faculty of Electronics and Computer Engineering, Universiti Teknikal Malaysia Melaka for their technical assistance in conducting the antenna measurements.

REFERENCES

[1] M. Ando, J. Takada, T. Numata, and N. Goto, "A linearly-polarized radial line slot antenna," in *1988 IEEE AP-S. International Symposium, Antennas and Propagation*, Syracuse, NY, USA: IEEE, vol. 2, pp. 836–839, 1988, doi: 10.1109/APS.1988.94209.

[2] M. Ando, T. Numata, J.-I. Takada, and N. Goto, "A linearly polarized radial line slot antenna," *IEEE Trans. Antennas Propagat.*, vol. 36, no. 12, pp. 1675–1680, Dec. 1988, doi: 10.1109/8.14389.

[3] M. E. Bialkowski and P. W. Davis, "A linearly polarized radial-line slot-array antenna with a broadened beam," *Microwave and Optical Technology Letters*, vol. 27, no. 2, pp. 98–101, 2000, doi: 10.1002/1098-2760(20001020)27:2<98::AID-MOP5>3.0.CO;2-Y.

[4] M. N. Y. Koli, M. U. Afzal, and K. P. Esselle, "Increasing the Gain of Beam-Tilted Circularly Polarized Radial Line Slot Array Antennas," *IEEE Trans. Antennas Propagat.*, vol. 70, no. 6, pp. 4392–4403, Jun. 2022, doi: 10.1109/TAP.2022.3140490.

[5] M. N. Y. Koli, M. U. Afzal, K. P. Esselle, and R. M. Hashmi, "An All-Metal High-Gain Radial-Line Slot-Array Antenna for Low-Cost Satellite Communication Systems," *IEEE Access*, vol. 8, pp. 139422–139432, 2020, doi: 10.1109/ACCESS.2020.3012787.

[6] M. Bertrand, M. Ettorre, G. Valerio, M. Albani, and M. Casaletti, "A Broadband Low-Profile Circularly Polarized Radial Line Slot Antenna," *IEEE Trans. Antennas Propagat.*, vol. 71, no. 1, pp. 140–150, Jan. 2023, doi: 10.1109/TAP.2022.3218761.

[7] O. Cumurcu, H. Torpi, and A. Caliskan, "Highly Efficient Circularly Polarized Radial Line Slot Array Antenna Using Non-Uniform Slot Density for 5G Communication System," *IEEE Access*, vol. 11, pp. 115688–115698, 2023, doi: 10.1109/ACCESS.2023.3325193.

[8] J. I. Herranz-Herruzo, A. Valero-Nogueira, M. Ferrando-Rocher, and B. Bernardo-Clemente, "High-Efficiency Ka-Band Circularly Polarized Radial-Line Slot Array Antenna on a Bed of Nails," *IEEE Trans. Antennas Propagat.*, vol. 70, no. 5, pp. 3343–3353, May 2022, doi: 10.1109/TAP.2021.3137376.

[9] K. L. Wolff, M. G. Bray, J. A. Schellhase, and C. Haskins, "Low Cost High Gain Antenna Fabrication and Testing for Mars EscaPADE," in *2023 United States National Committee of URSI National Radio Science Meeting (USNC-URSI NRSM)*, Boulder, CO, USA: IEEE, Jan. 2023, pp. 9–10, doi: 10.23919/USNC-URSINRSM57470.2023.10043140.

[10] M. Bray, "A Spiral Radial Line Slot Array Antenna for NASA's Double Asteroid Redirection Test (DART)," in *2020 IEEE International Symposium on Antennas and Propagation and North American Radio Science Meeting*, Montreal, QC, Canada: IEEE, Jul. 2020, pp. 379–380, doi: 10.1109/IEEECONF35879.2020.9330400.

[11] M. G. Bray, "Design, Development and Testing of NASA's DART Radial Line Slot Array Antenna," in *2023 United States National Committee of URSI National Radio Science Meeting (USNC-URSI NRSM)*, Boulder, CO, USA: IEEE, Jan. 2023, pp. 1–2, doi: 10.23919/USNC-URSINRSM57470.2023.10043116.

[12] E. Smith *et al.*, "Testing Early and Often: End-to-End Testing on the Double Asteroid Redirection Test (DART)," in *2020 IEEE Aerospace Conference*, Big Sky, MT, USA: IEEE, Mar. 2020, pp. 1–9, doi: 10.1109/AERO47225.2020.9172455.

[13] J. Hirokawa, K. Sakurai, M. Ando, and N. Goto, "Matching slot pair for a circularly-polarised slotted waveguide array," *IEE Proc. H Microw. Antennas Propag. UK*, vol. 137, no. 6, p. 367, 1990, doi: 10.1049/ip-h-2.1990.0066.

[14] T. Purnamirza *et al.*, "A design of radial line slot array antennas using the specification of panel antennas," *TELKOMNIKA (Telecommunication Computing Electronics and Control)*, vol. 17, no. 6, pp. 3066-3072, Dec. 2019, doi: 10.12928/telkomnika.v17i6.12679.

[15] T. Purnamirza, M. B. Poerwanto, D. Purwanto, M. I. Ibrahim, and D. Rahmi, "The technique to design multibeam Radial Line Slot Array (RLSA) antennas," *Journal of Electromagnetic Waves and Applications*, vol. 36, no. 5, pp. 626–636, Mar. 2022, doi: 10.1080/09205071.2021.1978332.

[16] T. Purnamirza, A. Nawawi, M. I. Ibrahim, and D. Rahmi, "The Utilization of Backgrounds as Radiating Elements to Construct Multibeam Radial Line Slot Array (RLSA) Antennas," *IRECAP*, vol. 11, no. 2, p. 118, Apr. 2021, doi: 10.15866/irecap.v11i2.20115.

[17] T. Purnamirza *et al.*, "Multibeam half radial line slot array (RLSA) antennas," *Electromagnetics*, vol. 43, no. 1, pp. 37–47, Jan. 2023, doi: 10.1080/02726343.2023.2177388.

[18] T. Purnamirza *et al.*, "Cutting Technique for Constructing Small Radial Line Slot Array Antennas," *J. Electromagn. Eng. Sci.*, vol. 21, no. 1, pp. 35–43, Jan. 2021, doi: 10.26866/jees.2021.21.1.35.

[19] H. Kim, T. H. Jang, and C. S. Park, "60-GHz Compact Vertically Polarized End-Fire Monopole-Based Yagi Antenna-in-Package for Wideband Mobile Communication," *IEEE Access*, vol. 10, pp. 111077–111086, 2022, doi: 10.1109/ACCESS.2022.3216264.

[20] L. Chen, Z.-Y. Lei, and X.-W. Shi, "Meander-Line Based Broadband Artificial Material for Enhancing the Gain of Printed End-Fire Antenna," *PIER*, vol. 151, pp. 55–63, 2015, doi: 10.2528/PIER15021401.

[21] B. Andres-Garcia, L. E. Garcia-Munoz, D. Segovia-Vargas, I. Camara-Mayorga, and R. Gusten, "Ultrawideband Antenna Excited by a Photomixer for Terahertz Band," *PIER*, vol. 114, pp. 1–15, 2011, doi: 10.2528/PIER11012513.

[22] H. Xu, B. Sima, P. Wei, L. Tang, S. Jiang, and C. Liu, "Millimeter Wave Planar Wideband Circularly Polarized Antenna Loaded Triangular Patch for End-Fire Radiation," *IEEE Access*, vol. 11, pp. 112569–112576, 2023, doi: 10.1109/ACCESS.2023.3323430.

[23] A. Dadgarpour, B. Zarghooni, B. S. Virdee, and T. A. Denidni, "Millimeter-Wave High-Gain SIW End-Fire Bow-tie Antenna," *IEEE Trans. Antennas Propagat.*, vol. 63, no. 5, pp. 2337–2342, May 2015, doi: 10.1109/TAP.2015.2406916.

[24] W. Zheng, S. Wang, M. Tang, G. Zhang, W. Ren, and C. Hua, "High-Permittivity Dielectric Half-Loop Yagi-Uda Antenna with End-Fire Radiation," *IEEE Open J. Antennas Propag.*, vol. 5, no. 1, pp. 180–189, Feb. 2024, doi: 10.1109/OJAP.2023.3340336.

[25] P. W. Davis and M. E. Bialkowski, "Experimental investigations into a linearly polarized radial slot antenna for DBS TV in Australia," *IEEE Trans. Antennas Propagat.*, vol. 45, no. 7, pp. 1123–1129, Jul. 1997, doi: 10.1109/8.596903.

BIOGRAPHIES OF AUTHORS

Teddy Purnamirza received his Bachelor degree from STTTelkom (currently Universitas Telkom) in 2000. He received his Master and Doctoral degree from UTM Malaysia, both in Electrical Engineering, in 2005 and 2013, respectively. He joined Department of Informatic Engineering, UIN Suska in 2000. From 2000 to 2003, he was head of informatics laboratory. He joined Department of Electrical Engineering, UIN Suska in 2003. From 2005 to 2007, he was Head of computer laboratory. From 2007 to 2010, he was Head of Department of Electrical Engineering in UIN Suska. From 2013 to 2018, he was Vice Dean for Academic Affairs and Institution Development at Faculty of Science and Technology UIN Suska. He is now serving as professor in UIN Suska. He has published three books, one chapter, twenty ones journal papers, and four conference papers. His research interests are antennas and propagations. He can be contacted at email: tptambusai@uin-suska.ac.id.

Junisbekov M. Shardarbekovich graduated from Lenin Kazakh Polytechnic Institute in 1974. He received his graduated degree from Moscow Textile Institute named after A.N. Kosygin at the Department of Automation and Industrial Electronics in 1982. In 1983, in December he defended his thesis for the degree of Candidate of Technical Sciences. He was Head of the Department of Automation and Electronics 1987-1991, Head of the Department of Technical Cybernetics 2001-2009, and was awarded the academic degree of professor of M.H. Dulati TarSU in 2005. He worked as director of the Institute of Postgraduate Education and Advanced Training since 2009 and as Head of the Department of "Technical Cybernetics 2010-2013". Since 2013, Head of the Department of Automation and Telecommunications. He was awarded honorary diplomas of the Ministry of Education, Mayor of Zhambyl region, Mayor of Taraz "Ulagatty Ustaz", honorary Worker of Education of the Republic of Kazakhstan, in 2009 he was awarded the title of "Best University Teacher". He is the author of 25 textbooks, 4 monographs and more than 150 scientific papers. He can be contacted at email: d_muhtar@mail.ru.

Riza A. Jaya was born in Pekanbaru, Riau, Indonesia on January, 25th, 1995. He received his Bachelor degree from Universitas Islam Negeri Suska Indonesia in Electrical Engineering in 2019. He worked at PT Kolega Energi Abadi from 2020 till 2022. He is now working at SUNterra Indonesia. He can be contacted at email: rizaadijaya17@gmail.com.

Imran Mohd Ibrahim is an Associate Professor at Universiti Teknikal Malaysia Melaka. He received his Bachelor, Master and Doctoral degree from Universiti Teknologi Malaysia, all in Electrical Engineering, in 2000, 2005, and 2016, respectively. He served as Faculty's Inaugural Deputy Dean (Research and Post Graduate Study) and contributed to the early development of research activities at faculty and institution. He has led several grants from industry, government and university in antenna research and wireless communication. He is also a committee member to IMT and Future Networks Working Group under Malaysia Technical Standard Forum Berhad. He also serves as drafter to the Technical Code, Prediction and Measurement of RF-EMF Exposure from Base Station. He has published more than 100 journals and conference papers. His research interests are antenna and microwave device design. He also supervised a Ph.D. and Master students by research in antenna design for beyond 5G and medical application. He was elevated to IEEE Senior Membership in 2021 based on his significant contribution in electrical and electronic engineering field. In January 2023, he has appointed as TVET ambassador for UTeM for the project Knowledge Transfer and Mobile Wi-fi Router Installation for Rural School Are. He can be contacted at email: imranibrahim@utem.edu.my.

Kabanbayev A. Batyrbekovich was born in Zhambil region, Zhanatas city, Kazakhstan, on December, 4th, 1987. He received his Bachelor degree and Master degree from Department of Electrical Engineering, Dulaty University in 2010 and 2011, respectively. He received his Doctoral degree from Karaganda Polytechnic University in 2020. He now served as Associate Professor in Department of Electrical Engineering, Dulaty University. He can be contacted at email: jogitama@gmail.com.

Depriwana Rahmi was born in Pasir Pangaraian, Riau, Indonesia on 6th March 1981. She received his Bachelor degree and Master degree from Universitas Riau and UTM Malaysia in 1999 and 2015, repectively. She joined Mathematic Education Department UIN Suska in 2006. She is now serving as senior lecturer in UIN Suska. She has published four books, eighteen journal papers and 4 conference papers. Her research interests are probability and statistics. She can be contacted at email: depriwanar@gmail.com.